

International Journal of Modern Physics D  
 © World Scientific Publishing Company

## BRANEWORLD BLACK HOLES IN COSMOLOGY AND ASTROPHYSICS

A. S. MAJUMDAR\*

N. MUKHERJEE†

*S. N. Bose National Centre for Basic Sciences  
 Block JD, Sector III, Salt Lake, Kolkata 700098, India*

Received Day Month Year

Revised Day Month Year

Communicated by Managing Editor

The braneworld description of our universe entails a large extra dimension and a fundamental scale of gravity that might be lower by several orders of magnitude compared to the Planck scale. An interesting consequence of the braneworld scenario is in the nature of spherically symmetric vacuum solutions to the brane gravitational field equations which could represent black holes with properties quite distinct compared to ordinary black holes in 4-dimensions. We discuss certain key features of some braneworld black hole geometries. Such black holes are likely to have diverse cosmological and astrophysical ramifications. The cosmological evolution of primordial braneworld black holes is described highlighting their longevity due to modified evaporation and effective accretion of radiation during the early braneworld high energy era. Observational abundance of various evaporation products of the black holes at different eras impose constraints on their initial mass fraction. Surviving primordial black holes could be candidates of dark matter present in galactic haloes. We discuss gravitational lensing by braneworld black holes. Observables related to the relativistic images of strong field gravitational lensing could in principle be used to distinguish between different braneworld black hole metrics in future observations.

*Keywords:* Branes, Black Holes, Cosmology, Gravitational Lensing

### 1. Introduction

There has been widespread activity in braneworld gravity in recent times<sup>1</sup>. The braneworld scenario of our universe opens up the fascinating possibility of the existence of large extra spatial dimensions by ensuring that the standard model fields are confined to the 3-brane, whereas gravity could also propagate into the higher dimensional bulk. Several braneworld models have been studied in the literature, the most popular among them being the Arkani-Hamed, Dimopoulos and Dvali (ADD) model<sup>2</sup>, and the two Randall-Sundrum (RS) models<sup>3,4</sup>. In the ADD model<sup>2</sup> there

\*e-mail:archan@bose.res.in

†e-mail:nupur@bose.res.in

could be  $n$  large compact extra dimensions with radius  $l$ , with  $n \geq 2$  providing a possible resolution of the hierarchy problem of particle physics. The RS-I model<sup>3</sup> is motivated from similar considerations and consists of two opposite tension branes, with our universe stipulated to be the negative tension brane. In the RS-II model<sup>4</sup> which has been the inspiration for an extensively developed braneworld cosmology<sup>5</sup>, the AdS5 bulk can have infinite size. Confinement of the standard model fields is achieved by a positive tension brane, and a negative cosmological constant for the AdS5 bulk with curvature radius  $l$ . The resultant modification of the Newtonian gravitational potential in braneworld models<sup>6,7</sup> is of the order  $1/r^3$  at distances  $r \geq l$  where  $l$  is the scale of the extra dimension(s). The failure of current experiments using torsion pendulums and mechanical oscillators to observe departures from Newtonian gravity at small scales have set the upper limit of  $l$  in the sub-millimeter region, i.e.,  $l \leq 0.2\text{mm}$ <sup>8</sup>.

It has been recently realized that the possibility of observing signatures of modified gravity in braneworld models with large extra dimensions exists in particle accelerator experiments. This is due to the fact that in braneworld gravity the fundamental 5-dimensional Planck scale  $M_5$  can be much below the 4-dimensional Planck scale  $M_4$ . If the scale of the extra dimension is not much below the limit obtained from table-top experiments<sup>8</sup>, then the corresponding  $M_5$  could be as high as the order of a TeV. Thus it is possible for mini 5-dimensional black holes to be produced in particle collisions with centre of mass energy of TeV order<sup>9</sup>. The production cross-sections of various higher dimensional black holes in future accelerators such as the LHC has been studied and possible signatures in the form of properties of end products of the Hawking evaporation from these black holes have been enlisted<sup>10</sup>. High energy cosmic ray showers could similarly produce small higher dimensional black holes, the possible signatures from which have also been studied<sup>11</sup>. It hence appears that observational signatures of braneworld gravity may be a distinct possibility in the near future from several avenues.

The analysis of gravitational field equations on the brane is conceptually complicated due to the fact that the propagation of gravity into the bulk does not permit the treatment of the brane gravitational field equations as a closed form system<sup>12</sup>. This makes the task of studying gravitational collapse on the brane rather difficult<sup>13</sup>. Garriga and Tanaka<sup>6</sup> first incorporated the effect of the Kaluza-Klein modes on the metric outside a spherically symmetric and static matter distribution on the brane in the form of the  $1/r^3$  correction to the gravitational potential. Since then though no exact solution of the full 5-dimensional bulk field equations have been found, various solutions representing braneworld black holes have been obtained based on different configurations for the projected 5-dimensional Weyl tensor on the brane. Among them the one of the Reissner-Nordstrom type with negative tidal charge<sup>14</sup> originating from the Weyl term has been discussed in details in the literature. The projection onto the brane of the 5-dimensional Schwarzschild solution given by the Myers-Perry metric<sup>15</sup> could effectively describe a small braneworld black hole of size  $r \leq l$ . The properties of such black holes have been investigated in details<sup>16</sup>.

The mechanism of Hawking evaporation has been formulated into the brane and the bulk as well<sup>17</sup>, and special features have been observed in the interaction of 5-dimensional black holes with branes<sup>18</sup>.

Braneworld black holes have been the subject of recent phenomenological interest in the arena of cosmology. Primordial black holes have potentially diverse ramifications on several eras of cosmological evolution. If braneworld black holes are formed in the early universe, their effect on subsequent dynamics could be not only varied but also widely different from those of primordial Schwarzschild black holes in standard cosmology. This is due to the reasons that braneworld black holes have different properties compared to ordinary 4-dimensional black holes, and also due to the entirely modified evolution of the very early stages of the universe in the braneworld scenario<sup>1,5</sup>. In particular, the Hubble expansion is modified by the presence of a term proportional to the square of the energy density on the right hand side of the Friedmann equation, which dominates the dynamics during the very early high energy phase. Primordial braneworld black holes that could be produced due to the collapse of horizon-sized density perturbations, have a lower temperature and evaporate slowly compared to the standard 4-dimensional black holes as a consequence of their different geometry<sup>19</sup>. Furthermore, the modified braneworld cosmological evolution of the universe enables accretion from the surrounding radiation to be effective towards increasing the mass and longevity of the black holes<sup>20,21</sup>. Primordial black holes could survive till many different eras in such a scenario, thereby contributing to the energy density of the universe. The Hawking evaporation products at the end of their life-cycles could have a significant bearing on several cosmological processes. Observational results such as the background gamma ray spectrum could hence be used to impose constraints on the initial mass spectrum of the black holes. These could be again significantly modified<sup>22</sup> compared to those that have been obtained for primordial Schwarzschild black holes in standard cosmology.

The prospect of survival of primordial black holes up to present times in the braneworld scenario naturally raises the question as to whether they could be a significant fraction of cold dark matter in galactic haloes, and also what role they could have in structure formation. In order to address these issues it is first important to obtain observational evidences of their existence and to determine their mass ranges. The two likely avenues for obtaining observational signatures from black holes that may be present in our galactic halo are through gravitational waves from coalescing black hole binaries, and through gravitational lensing of light sources by the black holes. It has been shown that energy exchange between neighbouring black holes that are formed in the high energy braneworld era facilitates the later formation of black hole binaries through gravitational interaction<sup>23</sup>. It has been also argued that binaries of primordial black holes in the braneworld scenario could emit gravitational waves observable by future detectors<sup>24</sup>. The study of gravitational lensing by braneworld black holes has been very recently undertaken. The deflection of light propagating on the brane due to bulk effects has been calculated<sup>25</sup>.

The expressions for the weak field bending angle of light in certain braneworld metrics has been obtained<sup>26</sup>. Further, the various lensing quantities for one possible braneworld black hole geometry have been obtained and compared to those for the Schwarzschild black hole in the weak field limit<sup>27</sup>. The richer phenomenology of strong field gravitational lensing such as the positions and magnifications of relativistic images is being investigated<sup>28</sup> in several braneworld geometries, and the values of observational parameters computed for a candidate lens<sup>29</sup>.

The plan of this review is as follows. In the next section we describe some candidate geometries for braneworld black holes. The arbitrariness of the projected bulk Weyl term on the brane is responsible for the existence of a number of possible solutions. We discuss some distinctive properties of a few of them. The aim of this article is to highlight the progress made in understanding the impact of having braneworld black holes in cosmological and astrophysical processes. In order to make this review a bit self-contained we provide a brief description of the essential features of the cosmology of the braneworld scenario in section 3. The stage is then set for a somewhat detailed analysis of the cosmological evolution of primordial braneworld black holes in section 4. Here we try to emphasize the key differences from the consequences of a population of primordial Schwarzschild black holes in standard cosmology. We begin section 5 with a skeletal description of the theoretical framework of gravitational lensing. We then present some recent results on braneworld lensing quantities and observables for some of the geometries described earlier. The underlying spirit here is the attempt to possibly discriminate between different gravity and braneworld gravity models by future observations. A summary is presented and some concluding remarks are made in section 6.

## 2. Spherically symmetric and static vacuum solutions on the brane

Obtaining the gravitational field due to a localised matter distribution on the brane has been an involved and challenging task right since the inception of braneworld models. This question is the forebearer of the problem of finding the final state of gravitational collapse on the brane, which is of central importance concerning the existence of black hole solutions in the braneworld scenario. The process of gravitational collapse in the braneworld scenario is much complicated compared to general relativity because in the former case whereas matter is confined to the brane, the gravitational field can also access the extra dimension. The corrections to the Newtonian potential of a point mass  $M$  at large distances due to the extra dimension were calculated to be<sup>3,6</sup>

$$V(r) = \frac{2M}{M_4^2 r} \left( 1 + \frac{2l^2}{3r^2} \right) \quad (1)$$

The failure of current experiments to detect such corrections at sub-millimeter scales have set the upper limit on the curvature radius  $l$  of the 5-th dimension as  $l \leq 0.2\text{mm}$ <sup>8</sup>.

The effect of Kaluza-Klein modes on the metric exterior to a static and spherically symmetric matter distribution on the brane was considered by Garriga and Tanaka<sup>6</sup>. They obtained a solution in the weak field limit given by

$$dS_4^2 = -\left(1 - \frac{2M}{M_4^2 r} + \frac{4Ml^2}{3M_4^2 r^3}\right)dt^2 + \left(1 + \frac{2M}{M_4^2 r} + \frac{2Ml^2}{3M_4^2 r^3}\right)(dr^2 + r^2 d\Omega^2) \quad (2)$$

Note that this solution is quite different from the Schwarzschild metric and that the gravitational potential obtained from this metric (2) has  $1/r^3$  corrections (1) compared to the Newtonian potential. Further perturbative studies<sup>7,30</sup> have also established that the first weak field correction to the Newtonian potential on the brane is proportional to  $1/r^3$ .

The projected Weyl term  $E_{\mu\nu}$  on the brane carries the imprint of Kaluza-Klein modes that could be relevant in the process of gravitational collapse. If the Weyl term vanishes, then the standard Schwarzschild solution in 4 dimensions can be assumed as the simplest black hole solution on the brane by ‘stacking’ it into the extra dimension. Such a vacuum solution of the 4-dimensional Einstein equation is of the ‘black string’ type<sup>31</sup>, and can be generalised to the case of a cosmological constant in 4 dimensions as well<sup>32</sup>. Subsequently, it was shown that the black string is unstable to large-scale perturbations<sup>33</sup>. Another solution to the vacuum 4-dimensional Einstein field equations is obtained by setting the 4-dimensional cosmological constant to zero (as in Eq.(16), thus obtaining a relation between the brane tension and the AdS radius (17)). Since the projected Weyl tensor on the brane is divergence free for the vacuum case, one gets for static solutions a closed system of equations given by<sup>12</sup>

$$\begin{aligned} R_{\mu\nu} &= -E_{\mu\nu} \\ R_{\mu}^{\mu} &= 0 \\ \nabla^{\mu} E_{\mu\nu} &= 0 \end{aligned} \quad (3)$$

Dadhich et al<sup>14</sup> have prescribed the mapping of the 4-dimensional general relativity solution with traceless energy momentum tensor of the Einstein-Maxwell type to a vacuum braneworld solution in 5 dimensions with the correspondence

$$\kappa^2 T_{\mu\nu} \leftrightarrow -E_{\mu\nu} \quad (4)$$

An exact black hole solution to the effective field equations on the brane of the Reissner-Nordstrom type was given with the above correspondence (4) as<sup>14</sup>

$$dS_4^2 = -\left(1 - \frac{2M}{M_4^2 r} + \frac{Q}{r^2}\right)dt^2 + \left(1 - \frac{2M}{M_4^2 r} + \frac{Q}{r^2}\right)^{-1}dr^2 + r^2(d\Omega^2) \quad (5)$$

where  $Q < 0$  is not the electric charge of the conventional Reissner-Nordstrom metric, but the negative ‘tidal charge’ arising from the projection on to the brane of the gravitational field in the bulk. Since the black hole mass  $M$  is the source of the bulk Weyl field, the tidal charge  $Q$  could be viewed as the reflection back on

the brane of the gravitational field of  $M$  by the negative AdS<sub>5</sub> bulk cosmological constant. In the limit  $r < l$ , it can be shown that<sup>14,34</sup>

$$Q = -\frac{Ml}{M_4^2} \quad (6)$$

The bulk tidal charge thus strengthens the gravitational field of the black hole. It has been further argued<sup>35</sup> that since the back reaction of the bulk onto the brane strengthens gravity on the brane, the formation of a black hole as result of gravitational collapse is favored as against a naked singularity. The metric with negative tidal charge (5) has a spacelike singularity and one horizon given by

$$r_h = \frac{M}{M_4^2} \left( 1 + \sqrt{1 - \frac{QM_4^4}{M^2}} \right) \quad (7)$$

which is larger than the Schwarzschild horizon. So the bulk effects are seen to increase the entropy and decrease the temperature of the black hole.

A more general class of spherically symmetric and static solutions to the field equations with a 5-dimensional cosmological constant can be derived by considering a general line element of the type

$$ds^2 = -A(r)dt^2 + B(r)dr^2 + r^2(d\Omega^2) \quad (8)$$

and relaxing the condition  $A(r) = B^{-1}(r)$  used while obtaining the Schwarzschild or the Reissner-Nordstrom metrics. Casadio et al<sup>36</sup> obtained two types of solutions by fixing either  $A(r)$  or  $B(r)$ , and then demanding the correct  $1/r$  asymptotic behaviour for the other in terms of the post Newtonian (PPN) parametrization. In the first case, the choice  $A(r) = 1 - 2M/(M_4^2 r)$  leads to the metric

$$ds_4^2 = -(1 - \frac{2M}{M_4^2 r})dt^2 + \frac{1 - \frac{3M}{2M_4^2 r}}{(1 - \frac{2M}{M_4^2 r}) \left( 1 - \frac{M(4\beta-1)}{2M_4^2 r} \right)} + r^2(d\Omega^2) \quad (9)$$

in terms of the PPN parameter  $\beta$  which impacts the deflection and time delay of light<sup>37</sup>. Note that the above metric was also derived as a possible geometry outside a star on the brane<sup>38</sup>. The solution (9) is of the temporal Schwarzschild form having a horizon  $r_h = 2M/M_4^2$ . The corresponding Hawking temperature is given by<sup>36</sup>

$$T_{BH} = \frac{\sqrt{1 - 6(\beta - 1)}}{8\pi M} \quad (10)$$

Thus, in comparison with Schwarzschild black holes, the black hole (9) will be either hotter or colder depending upon the sign of  $(\beta - 1)$ .

Alternately, the choice for  $B(r)$  of the form  $B^{-1}(r) = 1 - 2\gamma M/(M_4^2 r)$ , in terms of the PPN parameter  $\gamma$ , yeilds the line element

$$dS_4^2 = \frac{1}{\gamma^2} \left( \gamma - 1 + \sqrt{1 - \frac{2M}{M_4^2 r}} \right)^2 dt^2 + \frac{dr^2}{1 - \frac{2M}{M_4^2 r}} + r^2(d\Omega^2) \quad (11)$$

This form of the metric represents a nonsingular wormhole, and has been discussed earlier in the literature in the context of 4-dimensional general relativity<sup>39</sup>. Wormhole solutions in the braneworld context have been discussed by Bronnikov et al<sup>40</sup>. Furthermore, a class of static, spherically symmetric and non-singular braneworld solutions with horizon have been obtained<sup>41</sup> by relaxing the vanishing scalar curvature condition (3) used to obtain the solutions (5),(9) and (11). Stationary solutions representing charged rotating black holes have also been found recently<sup>42</sup>. The arbitrariness of the projected bulk Weyl term  $E_{\mu\nu}$  and its geometric origin is at the root of the variety of braneworld black hole and wormhole solutions since both the functions  $A(r)$  and  $B(r)$  in Eq.(8) have to be determined by it<sup>43</sup>. A specific configuration for the Weyl term with a negative equation of state has been considered and the resultant geometry with a singular horizon has been worked out to provide one more example of a possible braneworld black hole solution<sup>44</sup>.

The black hole solution (5) exhibits a  $1/r^2$  correction to the Newtonian potential on the brane in contrast to the weak field correction of  $1/r^3$  as in the solution (2). The solution with tidal charge (5) is reflective of the short distance or strong gravity limit where the  $1/r^2$  correction to the gravitational potential may even dominate over the  $1/r$ . This corresponds to the fact that at short distances, braneworld gravity is truly 5-dimensional. For short distances  $r \ll l$  it is natural to consider the 5-dimensional Schwarzschild solution as a braneworld black hole candidate given by<sup>15</sup>

$$ds_5^2 = - \left( 1 - \frac{r_{BH}^2}{r^2} \right) dt^2 + \left( 1 - \frac{r_{BH}^2}{r^2} \right)^{-1} dr^2 + r^2 (d\Omega_3^2) \quad (12)$$

where the horizon size  $r_0$  is so small ( $r_0 \ll l$ ) so that the black hole effectively “sees” all the spatial dimensions on the same footing. A generalisation to higher dimensions<sup>16,45</sup> of the hoop conjecture leads to the above form of the metric as a static solution to collapsing matter on the brane. Near the event horizon, the black hole would have no way of distinguishing between the bulk dimension and the braneworld ones. Numerical simulations for scales sufficiently small compared to the AdS scale  $l$  seem to also support the existence of static solutions satisfying the AdS5 boundary conditions<sup>46</sup>.

The induced 4-dimensional metric on the brane near the event horizon of the 5-dimensional black hole (12) is obtained by integrating out the extra dimension to be

$$ds_4^2 = - \left( 1 - \frac{r_{BH}^2}{r^2} \right) dt^2 + \left( 1 - \frac{r_{BH}^2}{r^2} \right)^{-1} dr^2 + r^2 (d\Omega^2) \quad (13)$$

This 4-dimensional metric is different from the standard 4-dimensional Schwarzschild solution as it reflects the 5-dimensional character of the strong gravitational field near the black hole horizon in the form of the  $1/r^2$  gravitational potential. It is however expected that far from the event horizon the metric (13) would approach the standard 4-dimensional Schwarzschild form, as was shown explicitly in 2+1 dimensional braneworld framework<sup>47</sup>. The properties of small black holes with

the geometry given by Eq.(13) have been studied extensively by Argyres et al<sup>16</sup>. In general these black holes have lesser temperature and a longer lifetime compared to the standard 4-dimensional Schwarzschild black holes. Also since the 5-dimensional Planck mass could be much lower compared to the 4-dimensional Planck mass ( $M_5 \ll M_4$ ), these black holes could be produced in particle accelerators<sup>9,10</sup> and cosmic ray showers<sup>11</sup>. They could thus provide one avenue of testing higher dimensional or braneworld physics. Of course, the consequences of a population of primordial black holes of the type (13) are potentially rich during many different cosmological eras, and these will be described in details in section 4.

The Myers-Perry black hole<sup>15</sup> in 5 dimensions (12) has been also used in the context of braneworld models to investigate various effects of its interaction with the brane and its radiation onto the bulk. Frolov and Stojkovic<sup>18</sup> have shown that a small black hole attached to the brane may leave the brane as the result of a recoil due to emission of quanta into the bulk. Such an effect leads to energy loss in the brane. This opens up the possibility of observing energy non-conservation in particle colliders which may be able to produce these black holes. Radiation by rotating 5-dimensional black holes have also been studied and certain conditions have been found when such objects could be stationary<sup>48</sup>. The interaction of 5-dimensional black holes with the brane described as a domain wall has interesting phenomenological features. In particular, the induced geometry on the brane due to a moving bulk black hole has been derived, and an apparent violation of the energy condition observed on the brane<sup>25</sup>. Specific features of the interaction of rotating black holes with the brane have been studied<sup>49</sup>. Energy flux through the horizons of various configurations of the black hole–domain wall system have also been investigated<sup>50</sup>.

Before concluding this section, it needs to be emphasized that although several spherically symmetric and static brane black hole solutions with contributions from the bulk gravity effects have been found<sup>14,36,38,41,43,44</sup>, and further possibilities have been elucidated as belonging to a more general class of black holes<sup>40</sup>, none of these are obtained as exact solutions of the full 5-dimensional bulk field equations. The analyses of gravitational collapse on the brane have typically yeilded non-static solutions<sup>13</sup>. Numerical simulations<sup>46,51</sup> have been inconclusive in this aspect. Investigations on stellar metrics<sup>43,52</sup> on the braneworld have been performed in order to obtain further insight into the full 5-dimensional spacetime geometry. Understanding the bulk properties have been attempted by extending some particular braneworld black hole solutions to the bulk<sup>53</sup>. The problem of finding the bulk metric which would represent a static and spherically symmetric vacuum solution with horizon on the brane remains an open one till date.

### 3. Braneworld cosmology

The cosmology of the RS-II model entails a modified high energy phase in the early radiation dominated era of the universe during which the right hand side of the

Einstein equation contains a term that is quadratic in the brane energy momentum tensor<sup>1</sup>. Other modifications include the so-called “dark-energy” term which is given by the projection of the bulk Weyl tensor. Transition to the standard radiation dominated era takes place when  $t >> t_c \equiv l/2$ . Such a modified high energy evolution has rich consequences for the physics of the early universe<sup>5</sup>. In particular, the inflationary scenario is altered, allowing the possibility of steep inflaton potentials to accomplish the desired features. Constraints on the duration of the brane dominated high energy phase are enforced by the necessity of conforming to the standard cosmological observational features such as nucleosynthesis and density perturbations.

Let us now review briefly some of the essential features of the RS-II braneworld cosmology. The effective 4-dimensional Einstein tensor on the brane is given by<sup>1</sup>

$$G_{\mu\nu} = \frac{8\pi}{M_4^2} \tau_{\mu\nu} + \kappa^4 \Pi_{\mu\nu} - E_{\mu\nu} \quad (14)$$

where  $\tau_{\mu\nu}$  is the brane energy-momentum tensor;  $\Pi_{\mu\nu}$  is quadratic in the brane EM tensor; and  $E_{\mu\nu}$  is the projection of the 5-dimensional Weyl tensor. The 4-dimensional Planck's mass  $M_4$  is related to the gravitational coupling constant  $\kappa$  and the AdS length  $l$  by  $\frac{8\pi}{M_4^2} = \frac{\kappa^2}{l}$ .

For the Friedmann-Robertson-Walker metric on the brane, the Friedmann equation is given by

$$H^2 = \frac{8\pi}{3M_4^2} \left( \rho + \frac{\rho^2}{2\lambda} + \rho_{KK} \right) + \frac{\Lambda_4}{3} - \frac{k}{a^2} \quad (15)$$

with  $H$  being the Hubble constant,  $\rho$  the energy density, and  $k = -1, 0, 1$  representing open, flat and closed branes, respectively.  $\rho_{KK}$  is the effective energy density coming from the bulk Weyl tensor,  $\lambda \equiv 3M_5^6/4\pi M_4^2$  is the brane tension, and  $\Lambda_4$  the effective 4-dimensional cosmological constant on the brane. The AdS curvature radius  $l$  is given by the bulk cosmological constant  $\Lambda_5$  and 5-dimensional Planck mass  $M_5$  as  $\Lambda_5 = -(3M_5^3)/(4\pi l^2)$ . The induced 4-dimensional cosmological constant  $\Lambda_4$  is given by

$$\Lambda_4 = 3 \left( \frac{M_5^6}{M_4^4} - \frac{1}{l^2} \right) \quad (16)$$

Setting  $\Lambda_4 = 0$ , one obtains a relation between the brane tension and AdS radius given by

$$\lambda^{-1/4} = \left( \frac{4\pi}{3} \right)^{1/4} \left( \frac{l}{l_4} \right)^{1/2} \quad (17)$$

Nucleosynthesis and CMBR observations constrain the “dark energy” term  $\rho_{KK}$  to be negligible compared to the radiation density  $\rho$ <sup>54</sup>. For much of cosmological evolution one can neglect  $\rho_{KK}$ , as we will do in the following analysis.

Assuming a radiation dominated equation of state, the ( $k = 0$ ) solutions for the Friedmann equation are given by

$$\rho_R = \frac{3M_4^2}{32\pi t(t + t_c)} \quad (18)$$

for the energy density, and

$$a = a_0 \left[ \frac{t(t + t_c)}{t_0(t_0 + t_c)} \right]^{1/4} \quad (19)$$

for the scale factor  $a$  during the radiation dominated era, and where  $t_c \equiv l/2$  effectively demarcates the brane dominated “high energy” era from the standard radiation dominated era. For times earlier than  $t_c$ , i.e.,  $t \leq t_c$  (or  $\rho \geq \lambda$ ), one has the non-standard high energy regime during which the radiation density and the scale factor evolve as

$$\rho_R = \frac{3M_4^2}{32\pi t_c t} \quad (20)$$

and

$$a = a_0 \left( \frac{t}{t_0} \right)^{1/4} \quad (21)$$

respectively. As a consequence, the time-temperature relation also gets modified during the brane dominated high energy era, i.e.,  $T \propto t^{-1/4}$ .

On the other hand, if the high energy braneworld regime is matter dominated from a time  $t_m$ , the scale factor grows subsequently like

$$a = a_m \left( \frac{t}{t_m} \right)^{1/3} \quad (22)$$

But, for times much later than  $t_c$ , i.e.,  $t \gg t_c$  (or  $\rho \ll \lambda$ ), one should recover back the standard radiation dominated cosmological evolution given by

$$\rho_R = \frac{3M_4^2}{32\pi t^2} \quad (23)$$

and

$$a = a_0 \left( \frac{t}{(t_0 t_c)^{1/2}} \right)^{1/2} \quad (24)$$

The observational success of standard big-bang nucleosynthesis constrains that the high energy era be over by the epoch of the synthesis of light elements. However, this requirement is satisfied for  $l < 10^{43} l_4$ , which is a much weaker bound than that obtained from experiments probing the modifications to Newtonian gravity<sup>8</sup> in the braneworld scenario.

Modified expansion in the high energy era has interesting implications for inflation<sup>55</sup>. For inflation driven by a scalar field  $\phi$  with potential  $V$  on the brane,

the condition for accelerated expansion of the scale factor ( $\ddot{a} > 0$ ) is satisfied when the equation of state parameter  $w$  is

$$w < -\frac{1}{3} \left( \frac{1+2\rho/\lambda}{1+\rho/\lambda} \right) \quad (25)$$

In the standard slow roll approximation the Hubble rate and the scalar field evolve as

$$H^2 \approx \frac{\kappa^2}{3} V \left( 1 + \frac{V}{2\lambda} \right) \dot{\phi} \approx \frac{V'}{3H} \quad (26)$$

The braneworld correction term  $V/2\lambda$  enhances the Hubble rate compared to standard cosmology. This in turn increases friction in the scalar field equation. Thus slow roll inflation is favored even for steep potentials<sup>56</sup>. The added advantage of such a scenario is that the inflaton field can play the role of quintessence<sup>57</sup> leading to a late time acceleration of the universe, as well. Further modifications to the high energy expansion in the very early stages can be brought about by the inclusion of the Gauss-Bonnet term in the 5-dimensional action<sup>58</sup>. During the very early era the Gauss-Bonnet term drives the Hubble rate as  $H^2 \propto \rho^{2/3}$  (Gauss-Bonnet regime), which subsequently changes to  $H^2 \propto \rho^2$  (Randall-Sundrum regime), and finally for  $t > t_c$  the  $H^2 \propto \rho$  (standard regime) evolution is recovered. Braneworld inflation could be accomplished by the Gauss-Bonnet term for very steep potentials such as the exponential potential<sup>59</sup>.

#### 4. Cosmological evolution of black holes

This section will focus on the consequences of a population of primordial black holes on cosmology in the braneworld scenario. The modified features of cosmology during the high energy braneworld era have been highlighted in section 2. The black holes present in the early universe affect the dynamics of the radiation dominated expansion through Hawking emission and accretion of the surrounding radiation<sup>20,21</sup>. These two competing processes lead to a net energy flow for a single black hole, the direction of which determines its longevity. The temperature and the rate of Hawking radiation for braneworld black holes are themselves different from those of standard 4-dimensional Schwarzschild black holes. The evolution of the individual black holes are impacted by the accretion of radiation from the surroundings, which is more effective in the braneworld scenario compared to the standard cosmology. Since the rate of accretion is governed by the rate of background expansion which is much slower in the high energy regime, black holes that are produced earlier undergo larger growth.

The actual rate of accretion and evaporation of course depends upon the particular geometry of the braneworld black hole. The black holes of interest for cosmological evolution are produced very early in the universe either due to the collapse of overdense regions resulting from inflation generated density perturbations, or due to the collision of heavy particles in the primordial plasma. Most of such black

holes are expected to be formed with a size small enough ( $r \leq l$ ) for the induced 4-dimensional Myers-Perry metric (13) to be a good approximation to their geometry on the brane. Further, as we are interested in the processes of Hawking evaporation and the accretion of radiation, both of which are characterized by the near horizon short distance properties of the metric, it may also be pragmatic to consider the 5-dimensional form of gravity reflected in the near horizon strong field region by the geometry in Eq.(13). It is worth noting that the collapse of the ‘tidal charge’ in vacuum could also give rise to the same geometry for primordial black holes<sup>14</sup> ( $M = 0$  in Eq.(5)). For these reasons only this particular form (13) of braneworld black hole geometry has been considered for the analysis of cosmological evolution<sup>19,20,21,22</sup>.

We first consider the evolution of a single primordial black hole which is formed with a sub-horizon mass<sup>19</sup> in the high energy radiation dominated era. Since we are considering the 4-dimensional projection of the 5-dimensional Schwarzschild metric, i.e.,

$$ds_4^2 = - \left(1 - \frac{r_{BH}^2}{r^2}\right) dt^2 + \left(1 - \frac{r_{BH}^2}{r^2}\right)^{-1} dr^2 + r^2 (d\Omega^2) \quad (27)$$

the horizon radius of such a black hole is proportional to the square root of its mass. The mass-radius relationship given by

$$r_{BH} = \left(\frac{8}{3\pi}\right)^{1/2} \left(\frac{l}{l_4}\right)^{1/2} \left(\frac{M}{M_4}\right)^{1/2} l_4 \quad (28)$$

which is different from the ordinary 4-dimensional Schwarzschild radius. Various properties of such black holes have been elaborated<sup>16</sup>, and the process of Hawking evaporation into the bulk and also on the brane have been extensively studied<sup>17</sup>. The Hawking evaporation rate, as for the case of standard black holes, is proportional to the surface area times the fourth power of temperature. The Hawking temperature is given by

$$T_{BH} = \frac{1}{2\pi r_{BH}} \quad (29)$$

Therefore, as a consequence of the mass-radius relationship (28), such black holes are colder and long-lived compared to 4-dimensional Schwarzschild black holes.

A black hole formed in the early radiation dominated era of the universe accretes the surrounding radiation. In standard cosmology the effectiveness of accretion in the growth of black hole mass is restricted because of the fact that the mass of the individual black holes could grow at nearly the same rate as that of the cosmological Hubble mass  $M_H$ , i.e.,  $M_H \sim M \sim t$ . Black holes produced in the radiation dominated era cannot be formed with a size much smaller than the Hubble radius, since otherwise pressure forces could hinder the collapse process. However, in the radiation dominated high energy phase of the braneworld scenario, the Hubble mass grows as  $M_H \sim t^2$ , whereas the growth of black hole mass due to accretion is given by  $M \sim t^B$  (with  $B < 2/\pi$ )<sup>20,21</sup>. Hence, sufficient energy is available within the

Hubble volume for a black hole to accrete in the high energy braneworld regime. The exact efficiency of accretion though depends upon complex physical processes involving the mean free paths of the particles comprising the radiation background and the thermal properties of the radiation in the non-trivial geometry near the event horizon<sup>21</sup>. Any peculiar velocity of the black hole with respect to the cosmic frame further impacts the rate of accretion. In the absence of a universally accepted approach of determining the precise accretion rate, it is usually taken to be as equal to the product of the surface area of the black hole, the energy density of the background radiation, and an efficiency factor ranging between 0 and 1<sup>21</sup>.

Taking into account these effects of accretion and evaporation together, the rate of change of mass  $\dot{M}$  of a braneworld black hole is given by

$$\dot{M} = 4\pi r_{BH}^2 \left( -g_{brane} \sigma T_{BH}^4 + f \rho_R \right) \quad (30)$$

where  $g_{brane}$  is effective number of particles that can be emitted by the black hole (we assume that the black holes can emit massless particles only and take  $g_{brane} = 7.25^{19}$ ),  $f$  is the accretion efficiency ( $0 \leq f \leq 1$ )<sup>21</sup>, and  $\sigma$  is the Stefan-Boltzmann constant. The black hole also evaporates into the bulk, with a rate proportional to  $4\pi r_{BH}^2 g_{bulk} T_{BH}^5$ . However, this term is subdominant even for very small black holes<sup>19</sup>, and has negligible effect on their lifetimes.

Substituting the expressions for the black hole radius (Eq.(28)), the temperature-radius relation (29), and the energy density of radiation (20), the black hole rate equation (30) in the radiation dominated high energy braneworld era can be written as<sup>20</sup>

$$\dot{M} = -\frac{AM_4^2}{Mt_c} + \frac{BM}{t} \quad (31)$$

where  $A$  and  $B$  are dimensionless numbers given by

$$A \simeq \frac{3}{(16)^3 \pi} \quad (32)$$

$$B \simeq \frac{2f}{\pi} \quad (33)$$

The exact solution for the black hole rate equation is given by<sup>20</sup>

$$M(t) = \left[ \left( M_0^2 - \frac{2AM_4^2}{2B-1} \frac{t_0}{t_c} \right) \left( \frac{t}{t_0} \right)^{2B} + \frac{2AM_4^2}{2B-1} \frac{t}{t_c} \right]^{1/2} \quad (34)$$

with  $M_0$  being the formation mass of the black hole at time  $t = t_0$ . If the black hole is formed out of the collapse of horizon or sub-horizon sized density perturbations, the formation time and mass are related by<sup>19</sup>

$$\frac{t_0}{t_4} \simeq \frac{1}{4} \left( \frac{M_0}{M_4} \right)^{1/2} \left( \frac{l}{l_4} \right)^{1/2} \quad (35)$$

It has been argued<sup>20</sup> that a black hole so formed continues to grow in size by the accretion of radiation during the high energy radiation dominated era, with its mass increasing as

$$\frac{M(t)}{M_0} \simeq \left( \frac{t}{t_0} \right)^B \quad (36)$$

This result is however sensitive to the accretion efficiency, since a more careful analysis<sup>21</sup> shows that for  $f < \pi/4$ , the growth due to accretion could come to a halt during the high energy regime itself.

Within the context of standard cosmology, the evolution of a population of primordial black holes exchanging energy with the surrounding radiation by accretion and evaporation has been studied by several authors<sup>60,61</sup>. The analysis of this problem is simplified by assuming that all the black holes are formed with an average initial mass  $M_0$  at a time  $t_0$  when the fraction of the total energy density in black holes is  $\beta_{BH}$ , and the number density of black holes is  $n_{BH}(t_0)$ . With these assumptions, the coupled cosmological equations for the radiation density  $\rho_R(t)$ , the matter density in the black holes  $M(t)n_{BH}(t)$ , and the scale factor  $a(t)$  are integrated to give the complete cosmological evolution. Note however, that the black holes are produced with an initial mass spectrum in any realistic scenario of black hole formation in the standard cosmology<sup>62</sup>, and it is expected that the same would be the case in the braneworld scenario as well. The effect of a mass distribution can be incorporated into the cosmological evolution in the standard scenario by introducing an additional differential equation for the distribution function and specifying further initial conditions related to it<sup>61</sup>. However, since not much is known about the formation processes of black holes in braneworld cosmology, the study of only a few basic features of their cosmological evolution under simplifying assumptions has been undertaken in the literature till date.

The number density of black holes  $n_{BH}(t)$  scales as  $a(t)^{-3}$ , and thus for a radiation dominated evolution on the brane, one gets

$$(n_{BH}(t)/n_{BH}(t_0)) = (t_0/t)^{3/4} \quad (37)$$

since  $a(t) \propto t^{1/4}$ . The net energy in black holes grows since accretion dominates over evaporation. The condition for the universe to remain radiation dominated (i.e.,  $\rho_{BH}(t) < \rho_R(t)$ ) at any instant  $t$  can be derived to be<sup>20</sup>

$$\beta_{BH} < \frac{(t_0/t)^{B+1/4}}{1 + (t_0/t)^{B+1/4}} \quad (38)$$

If the value of  $\beta_{BH}$  exceeds the above bound, there ensues an era of matter (black hole) domination in the high energy braneworld phase. Such a phase of matter domination should definitely be over by the time of nucleosynthesis for the cosmology to be viable.

Let us first describe the situation when the cosmology stays radiation dominated up to the time when brane effects are important, i.e.,  $t \leq t_c$ . From Eq.(38), this requires

$$\frac{\beta_{BH}}{1 - \beta_{BH}} < \left( \frac{t_0}{t_c} \right)^{B+1/4} \quad (39)$$

Further, the black holes should remain small enough, i.e.,  $(M/M_4) < (3\pi/4)(t/t_4)$  for the 5-dimensional evaporation law to be valid<sup>19</sup>. These criteria can be used to put an upper bound to the average initial mass<sup>20</sup>

$$\frac{M_0}{M_4} < \left( \frac{3\pi}{4(2\sqrt{2})^B} \right)^{\frac{2}{2-B}} \frac{t_c}{t_4} \quad (40)$$

The growth of the black holes in the radiation dominated era due to accretion slows down with time, since the surrounding radiation density gets diluted. The rate of evaporation is also insignificant for a wide range of  $M_0$  at this stage since the black hole masses could have grown by several orders of magnitude from their initial values. There ensues an era during which the black hole mass stays nearly constant over a period of time, as is the case for standard cosmology<sup>60</sup>. The accretion rate is smaller for the braneworld case since the surface area is proportional to  $M$  instead of  $M^2$  for 4-dimensional black holes. Moreover, the evaporation rate is ( $\propto M^{-1}$ ) instead of  $M^{-2}$ . Hence, the black hole mass will stay for while near a maximum value  $M_{max}$  reached at time  $t_t$  before evaporation starts dominating. The expression for the lifetime  $t_{end}$  of a black hole in this scenario is given by<sup>20</sup>

$$\frac{t_{end}}{t_4} \simeq \frac{4}{A} (2\sqrt{2})^B \left( \frac{M_0}{M_4} \right)^{2-B} \frac{t_c}{t_4} \left( \frac{t_t^2}{t_c t_4} \right)^B \quad (41)$$

It is important to note that the modified evaporation law also contributes to the increased lifetime for braneworld black holes<sup>19</sup>. However, the effect of accretion is more significant, as can be seen by comparing the lifetime of a 5-dimensional black hole in the presence of accretion to the the lifetime due to purely an altered geometry<sup>20</sup>. Depending upon the values taken by the parameters  $t_c$  and  $l$ , one could obtain several interesting examples of primordial black holes surviving till various cosmologically interesting eras<sup>20,21</sup>. One particular choice worth mentioning is that of a black hole formed with an initial mass  $M_0 = 10^8 M_4 \simeq 10^3 g$ , that will survive up to the present era if one chooses  $(l/l_4) \simeq 10^{30}$ .

Further interesting phenomena occur in the interaction of two or more neighbouring black holes mediated by the surrounding radiation in the radiation dominated high energy era. These black holes exchange energy via the processes of evaporation and accretion with the radiation bath, and through it, with each other. The evolution equation for a black hole gets modified due to the presence of one or more neighbouring black hole(s) with the addition of an extra source (sink) term due

to the evaporating (accreting) neighbour(s) over the average radiation background. The black hole equation (31) now becomes

$$\dot{m}_i = \frac{Bm_i}{\tilde{t}} - \frac{1}{m_i} - g \frac{m_i \dot{m}_j}{\tilde{t}^{1/2}} \quad (42)$$

where  $\tilde{t} = Am_4^2 t/t_c$ , and

$$g = \frac{4A^{1/2}}{3\pi} \left( \frac{l_4}{d_0} \right)^2 \left( \frac{t_0}{t_4} \right)^{1/2} \left( \frac{t_c}{t_4} \right)^{1/2} \quad (43)$$

can be dubbed as the ‘coupling’ parameter between two black holes. The physical distance between two such neighbours increases initially with the Hubble expansion. Forming out of horizon collapse, the initial mass ratio of two such black holes is on average proportional to the square of the ratio of the ratio of their formation times (from Eq.(35)). By studying the effect of the interaction term it is possible to show that an initial mass difference between two such black holes can never decrease during the radiation dominated era<sup>23</sup>.

The energy exchange between the black holes and the surrounding radiation always causes mass disequilibration between neighbours. Such mass differences facilitate the formation of binaries during the standard low energy phase via three-body gravitational interactions. A formation mechanism for primordial black hole binaries in standard cosmology has been investigated<sup>63</sup> which shows that if equal mass primordial black holes are inhomogeneously distributed in space, three-body gravitational interactions could lead to the formation of binaries. The scheme of binary formation in the braneworld scenario<sup>23</sup> could become more effective when combined with the scheme based on spatial inhomogeneities discussed in the context of standard cosmology<sup>63</sup>. Coalescing braneworld black hole binaries may emit gravitational waves amenable for detection by the next generation detectors<sup>24</sup>.

Let us now describe the case of matter (black hole) domination in the high energy phase. The onset of such a matter dominated era is derived to be<sup>20</sup>

$$\frac{t_{heq}}{t_0} = \left( \frac{1 - \beta_{BH}}{\beta_{BH}} \right)^{\frac{4}{4B+1}} \equiv \gamma_B \quad (44)$$

The mass of a black hole at  $t_{heq}$  is given by  $M(t_{heq}/M_0) = \gamma_B^B$ . For  $t > t_{heq}$  the Hubble expansion is essentially driven by the black holes ( $p = 0$ ) which dominate over radiation. Since the number density of black holes scales as matter ( $n_{BH}(t) \propto a^{-3}$ ), for  $t < t_c$  one has  $H \propto \rho_{BH}$ , and thus the scale factor grows as

$$a(t) \sim t^{1/3} \quad (45)$$

During this era, the radiation density  $\rho_R$  is governed by the equation

$$\frac{d}{dt} \left( \rho_R(t) a^4(t) \right) = -\dot{M}(t) n_{BH}(t) a(t) \quad (46)$$

where the contribution from accreting black holes is comparable to the normal redshifting term ( $\rho_R \sim a^{-4}$ ) because at this stage the black holes dominate the

total energy density. Some further analysis leads to the following expression for the radiation density<sup>20</sup>

$$\rho_R(t) \approx \gamma_B^{-1} \rho(t_0) \left( \frac{t_{heq}}{t} \right) - \frac{\beta_{BH} B}{B + 1/3} \gamma_B^{1/4} \rho(t_0) \left( \frac{t_0}{t} \right)^{1-B} \quad (47)$$

The black hole mass grows as

$$M(t) = M_0 \gamma_B^B \exp \left[ 3B + \frac{C}{B} \gamma_B^{B+1/4} - 3B \left( \frac{t_{heq}}{t} \right)^{1/3} - \gamma_B^{1/4} \frac{C}{B} \left( \frac{t}{t_0} \right)^B \right] \quad (48)$$

where  $C = \frac{\beta_{BH} B}{B + 1/3}$ . As in the case of standard cosmology, the accretion regime lasts for a brief duration in the matter dominated phase, beyond which the black hole evaporation starts to play a significant role.

The universe gets reheated as  $\rho_R(t)$  increases with time. The stage of black hole domination lasts up to a time  $t_r$  ( $\rho_R(t_r) = n_{BH}(t_r)M(t_r)$ ). Subsequently, radiation domination takes over once again. One can derive<sup>20</sup>

$$\frac{t_c}{t_r} \approx \frac{3}{2\delta_B \gamma_B} + \frac{A}{4\gamma_B^{2B}} \left( \frac{M_4}{M_0} \right)^2 \quad (49)$$

with

$$\delta_B \equiv \left( \frac{B + 1/3}{1 - \beta_{BH}} \right)^{\frac{3}{3\beta_{BH} + 1}} \quad (50)$$

A stringent restriction is imposed by demanding that the standard low energy cosmology (for  $t > t_c$ ) should emerge as radiation dominated. By requiring that the era of black hole domination be over before  $t_c$ , i.e.,  $t_r < t_c$ , one gets a lower bound on  $\beta_{BH}$  from Eq.(35), i.e.,

$$\beta_{BH} \geq \left[ \frac{4t_0}{3t_c} (B + 1/3)^{\frac{3}{3B+1}} \right]^{B+1/4} \quad (51)$$

The evaporation time of black holes in this scenario has also been calculated<sup>20</sup>. The black hole lifetime is given by

$$\frac{t_{end}}{t_4} \approx \left( \frac{M_0}{M_4} \right)^2 \frac{t_c}{t_4} \gamma_B^{2B} \quad (52)$$

The effect of accretion is less significant in prolonging black hole lifetimes in this case, as borne out by the following example. For instance, taking the value of the AdS radius to be  $l/l_4 \simeq 10^{20}$ , and  $\beta_{BH} = 10^{-3}$ , black holes with  $M_0 \simeq 10^{12} g$  evaporate during the present era. This is only to be expected, since early matter domination results in larger Hubble expansion rate which further restricts the availability of radiation for the black holes to accrete.

It thus turns out that it is possible to have primordial black holes formed in the high energy era of the braneworld scenario to survive up to several cosmologically interesting eras. Accretion of radiation during the radiation dominated era is primarily responsible for the increased longevity of braneworld black holes, though their 5-dimensional geometry also contributes to a slower rate of Hawking evaporation. It is worth noting here that primordial black holes in certain models could also accrete the energy of a cosmological scalar field<sup>64</sup>. Such an effect could lead to further growth of these black holes beyond the early radiation dominated era, thus pushing up their lifetimes further. The implications for a population of primordial black holes in cosmology are diversely manifold. At any particular era, the surviving black holes would contribute a portion to the the total energy density as dark matter in the universe. If the black holes are produced with an initial mass spectrum, then one would have evaporating black holes at different eras. Hawking radiation from these evaporating black holes would on one hand produce all kinds of particles including heavier ones which could lead to baryogenesis<sup>60</sup>, and on the other, could contribute significantly to the background photons, thus diluting the baryon to photon ratio.

Observational constraints impacting different cosmological eras could be used to impose restrictions on the initial mass spectrum of braneworld black holes in a manner similar to the primordial black holes in standard cosmology. Clancy et al<sup>22</sup> have shown how standard constraints are modified in the case of braneworld cosmology. To simplify the treatment, one can assume that radiation domination persists up to  $t_c$ , and that the accretion of radiation is possible only up to  $t_c$ . A black hole mass fraction  $\alpha_M$  in terms of the radiation density can be defined (related to the mass fraction  $\beta_{BH}$ ) as

$$\begin{aligned}\alpha_{M_0}(t) &= \frac{\rho_{BH}(t)}{\rho_T} \\ \alpha_{M_0}(t_0) &= \frac{\beta_{BH}}{1 - \beta_{BH}}\end{aligned}\tag{53}$$

Similarly, a ‘final’ mass fraction  $\alpha(t_{\text{evap}})$  is defined at the end of the black hole life-cycle, since the black holes radiate most of their energy towards the very end of their lifetimes. Observational constraints on  $\alpha(t_{\text{evap}})$  are considered at different cosmological epochs, given by

$$\alpha(t) < L_{4D}(t)\tag{54}$$

for standard 4-dimensional black holes, or

$$\alpha(t) < L_{5D}(t)\tag{55}$$

for braneworld black holes. Then these constraints are evolved backwards to constrain initial mass spectrum. Accretion in the high-energy phase leads to  $\alpha(t) \propto M_{BH}(t)a(t)$ . Therefore the constraints on the initial black hole mass fraction are

given by

$$L_{4D}^0 \equiv \alpha_i < \left[ \frac{a_0}{a(t)} \right]_{4D} L_{4D}(t) \quad (56)$$

for standard cosmological evolution, and

$$L_{5D}^0 \equiv \alpha_i < \left[ \frac{a_0}{a(t)} \right]_{5D} L_{5D}(t) \quad (57)$$

in the braneworld scenario. Any astrophysical or cosmological process to be constrained at certain epoch is dominantly affected by the PBHs with lifetimes of that epoch. The constraints on primordial black holes in standard cosmology thus get modified to<sup>22</sup>

$$\frac{L_{5D}^0}{L_{4D}^0} = \frac{L_{5D}(t_{\text{evap}})}{L_{4D}(t_{\text{evap}})} \left( \frac{l}{l_{\min}} \right)^{\frac{5-16B}{16-8B}} \quad (58)$$

where  $l_{\min} \propto t_{\text{evap}}^{1/3}$ . The departure from standard constraints is sensitive to the accretion efficiency, as is expected.

A more detailed study on how the initial mass spectrum of the black holes is distorted due to braneworld accretion has been undertaken by Sendouda et al<sup>65</sup>. The diffuse photon background emitted by the spectrum of black holes has been shown to be modified in accordance with the mass spectrum of the black holes. These results have been compared to the observed diffuse photon background to obtain bounds on the initial black hole mass fraction, the scale of the extra dimension, and the accretion efficiency by these authors. The observed number density of massive particles could also be used to obtain bounds on the initial mass fraction of the black holes, as in the case of Schwarzschild primordial black holes in standard cosmology. Further constraints on the scale of the extra dimension have been derived<sup>66</sup> by considering the recent observation of sub-Gev galactic antiprotons<sup>67</sup> as originating from braneworld black holes present in our galaxy. A relevant issue is to investigate whether primordial braneworld black holes could contribute to a significant fraction of cold dark matter. If so, the direct searches of cold dark matter compact objects through gravitational lensing might be able to reveal their presence in galactic haloes. In the next section we will report on the specific features of the analysis of gravitational lensing for several braneworld black hole metrics.

## 5. Gravitational lensing by braneworld black holes

The braneworld scenario implies the modification of Einstein's general relativity at short distances or strong gravitational fields. The bending of light due to the gravitational potential of a massive object is one of the first predictions of the general theory of relativity. Its application in the phenomenon of gravitational lensing<sup>68</sup> has potentially diverse possibilities. Gravitational lensing in the weak field limit<sup>69</sup> is till date one of the most widely used tool in observational astrophysics and cosmology. On the other hand, strong field gravitational lensing, though limited in observational utility because of presently inadequate instruments, remains our ultimate

scope for exploring the physics of strong gravitational fields. The general technique for analysing strong gravitational lensing for spherically symmetric metrics has been developed by Bozza<sup>70,71</sup> who has also formulated useful connections between observational quantities like fluxes and resolutions and the metric parameters. Strong gravitational lensing is also endowed with richer phenomenological features like relativistic images<sup>72,73</sup> and retrolensing<sup>74,75,76</sup>. It would be thus worthwhile to investigate if the results of strong gravitational lensing could be used for probing the modifications to general relativity made in braneworld geometries. Such studies are also motivated from the possibility of producing braneworld black holes in future accelerators<sup>9,10</sup>.

Analysis of the trajectories of light and massive particles in various braneworld and higher dimensional metrics have been undertaken recently. Kar and Sinha<sup>26</sup> obtained the bending angle of light for several brane and bulk geometries. Frolov et al<sup>78</sup> found certain non-trivial features about the propagation of light in the Myers-Perry<sup>15</sup> metric for a 5-dimensional black hole solution. This solution represents primordial black holes that could be produced with size  $r < l$  in the early high energy era of the RS-II braneworld scenario<sup>19</sup>. It was shown that such black holes could grow in size due to accretion of radiation, and consequently survive till much later stages in the evolution of the universe<sup>20</sup>. With a suitable choice of parameters, some of these black holes could also exist in the form of coalescing binaries in galactic haloes at present times<sup>23</sup>. The weak field limit of gravitational lensing was studied for the Myers-Perry metric and certain notable differences from the standard Schwarzschild lensing were found<sup>27</sup>. Thereafter, Eiroa<sup>28</sup> analysed the strong field lensing and retrolensing effects for the Myers-Perry black hole. Strong field gravitational lensing in a couple of other braneworld metrics has been discussed by Whisker<sup>29</sup> and some lensing observables have been computed using parameters for the galactic centre black hole.

For a spherically symmetric metric

$$ds^2 = -A(r)dt^2 + B(r)dx^2 + C(r)(d\Omega^2) \quad (59)$$

where the asymptotic forms of the functions  $A(r)$  and  $B(r)$  have the standard  $1/r$  form, and  $C(r) \rightarrow r^2$  asymptotically, the general formalism of strong field gravitational lensing has been worked out by Bozza<sup>71</sup>. It is required that the equation

$$\frac{C'(r)}{C(r)} = \frac{A'(r)}{A(r)} \quad (60)$$

admits at least one positive solution the largest of which is defined to be the photon sphere  $r_{ph}$ .

A photon emanating from a distant source and having an impact parameter  $u$  will approach near the black hole at a minimum distance  $r_0$  before emerging in a different direction (see Figure 1). The closest approach distance is given in terms of the impact parameter by

$$u = \sqrt{\frac{C_0}{A_0}} \quad (61)$$

where the functions  $C$  and  $A$  are evaluated at  $r_0$ . The deflection angle of the photon in terms of the distance of closest approach is

$$\alpha(r_0) = I(r_0) - \pi \quad (62)$$

$$I(r_0) = \int_{r_0}^{\infty} \frac{2\sqrt{B}dr}{\sqrt{C} \sqrt{\frac{C}{C_0} \frac{A_0}{A} - 1}} \quad (63)$$

The weak field limit is obtained by expanding the integrand in Eq.(63) to the first order in the gravitational potential. This limit however is not a good approximation when there is a significant difference between the impact parameter  $u$  and the distance of closest approach  $r_0$ , which occurs when  $A(r_0)$  significantly differs from 1, or  $C(r_0)$  from  $r_0^2$ . By decreasing the impact parameter, and consequently the distance of closest approach, the deflection angle increases beyond  $2\pi$  at some stage resulting in one or more photonic loops around the black hole before emergence. Further decrease of the impact parameter to a minimum value  $u_m$  corresponding to the distance of closest approach  $r_0 = r_{ph}$  results in the divergence of the deflection angle (integral in Eq.(63)), which means that the photon is captured by the black hole. Strong field gravitational lensing is useful for studying the deflection of light in a region starting from just beyond the photon sphere up to the distance where the weak field approximation approaches validity.

In the general analysis of strong field gravitational lensing it becomes necessary to extract out the divergent part of the deflection angle. In order to do so two new variables  $y$  and  $z$  are defined as<sup>71</sup>

$$y = A(r) \quad (64)$$

$$z = \frac{y - y_0}{1 - y_0} \quad (65)$$

where  $y_0 = A_0$ . In terms of these variables, the integral (63) in the deflection angle is given by

$$I(r_0) = \int_0^1 R(z, r_0) f(z, r_0) dz \quad (66)$$

$$R(z, r_0) = \frac{2\sqrt{By}}{CA'} (1 - y_0) \sqrt{C_0} \quad (67)$$

$$f(z, r_0) = \frac{1}{\sqrt{y_0 - [(1 - y_0)z + y_0] \frac{C_0}{C}}} \quad (68)$$

where all functions without the subscript 0 are evaluated at  $r = A^{-1}[(1 - y_0)z + y_0]$ . The function  $R(z, r_0)$  is regular for all values of  $z$  and  $r_0$ , while  $f(z, r_0)$  diverges for  $z \rightarrow 0$ .

The deflection angle can be written as a function of  $\theta = u/D_d$ , where  $\theta$  is the angular separation of the image from the lens, and  $D_d$  is the distance between the

lense and the observer (See Figure 1). In order to do so, an integral

$$b_R = \int_0^1 g(z, r_m) dz \quad (69)$$

is defined, where

$$g(z, r_m) = R(z, r_m) f(z, r_m) - R(0, r_m) f_0(z, r_m) \quad (70)$$

The expression for the deflection angle is given as a function of  $\theta = u/D_d$  as<sup>71</sup>

$$\alpha(\theta) = -\bar{a} \log \left( \frac{\theta D_d}{u_m} - 1 \right) + \bar{b} \quad (71)$$

$$\bar{a} = \frac{R(0, r_m)}{2\sqrt{\beta_m}} \quad (72)$$

$$\bar{b} = -\pi + b_R + \bar{a} \log \frac{2\beta_m}{y_m} \quad (73)$$

where  $R(0, r_m)$  and  $b_R$  are given be Eqs.(67) and (69), respectively, and  $\beta_m$  is defined as

$$\beta_m = \frac{C_m (1 - y_m)^2 (C_m'' y_m - C_m A''(r_m))}{2y_m^2 C_m'^2} \quad (74)$$

In strong lensing there may exist  $n$  relativistic images given by the number of times a light ray loops around the black hole. The positions of these are obtained as solutions of the lense equation given by

$$\tan \delta = \tan \theta - \frac{D_{ds}}{D_s} [\tan \theta + \tan(\alpha - \theta)] \quad (75)$$

for specific positions of the source and the lense respective to the observer, and using the the value of the deflection angle from Eq.(71). The relativistic images formed by light rays winding around the black hole are highly demagnified compared to the

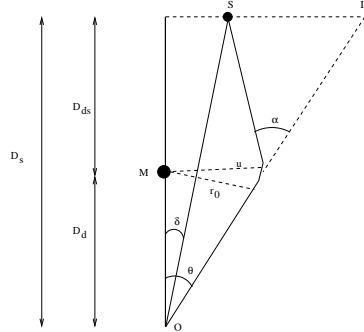


Fig. 1. Gravitationl lensing for point like mass object *M*. A light ray from the source *S* passes the lense with an impact parameter *u*, and is deflected by an angle  $\alpha$ . The observer sees an image *I* of the source at the angular position  $\theta$ .

weak field images. When the source, the lense and the observer are highly aligned, it is possible to obtain the most prominent of the relativistic images<sup>72</sup>. Hence, the analysis of strong lensing is usually restricted to the case when both  $\delta$  and  $\theta$  are small<sup>71</sup>, though the general case for arbitrary positions can also be analysed<sup>76</sup>. With the above restriction on the values of  $\delta$  and  $\theta$ , a light ray will reach the observer after winding around the lense  $n$  number of times only if the deflection angle  $\alpha$  is very close to a multiple of  $2\pi$ . Substituting  $\alpha = 2n\pi + \Delta\alpha_n$  in Eq.(75), one gets

$$\delta = \theta - \frac{D_{ds}}{D_s} \Delta\alpha_n \quad (76)$$

The position of the  $n$ -th relativistic image  $\theta_n$  can hence be obtained as a solution of the lense equation (76) as<sup>71</sup>

$$\theta_n = \frac{u_m}{D_d} (1 + e_n) + \frac{u_m e_n \left( \delta - \frac{u_m (1 + e_n)}{D_d} \right) D_s}{\bar{a} D_{ds} D_d} \quad (77)$$

where  $u_m$  is the minimum impact parameter, and  $e_n$  is given by

$$e_n = e^{(\bar{b} - 2n\pi)/\bar{a}} \quad (78)$$

The magnification  $\mu_n$  of the  $n$ -th relativistic image is given by<sup>71</sup>

$$\mu_n = \frac{1}{(\delta/\theta) \partial \delta \partial \theta} \Big|_{\theta_n} \simeq \frac{u_m^2 e_n (1 + e_n) D_s}{\bar{a} \delta D_{ds} D_d^2} \quad (79)$$

The above formula for magnification is valid under the approximation of a point source. However, for an extended source the magnification at the image positon can also be derived by integrating over the luminosity profile of the source<sup>75</sup>.

It is useful to obtain the expressions for the various lensing observables in terms of the metric parameters. For  $n \rightarrow \infty$  an observable  $\theta_\infty$  can be defined<sup>71</sup> representing the asymptotic position approached by a set of images. The minimum impact parameter can then be obtained as

$$u_m = D_d \theta_\infty \quad (80)$$

In the simplest situation where only the outermost image  $\theta_1$  is resolved as a single image, while all the remaining ones are packed together at  $\theta_\infty$ , two lensing observables can be defined as<sup>71</sup>

$$\mathcal{S} = \theta_1 - \theta_\infty \quad (81)$$

representing the separation between the first image and the others, and

$$\mathcal{R} = \frac{\mu_1}{\sum_{n=2}^{\infty} \mu_n} \quad (82)$$

corresponding to the ratio between the flux of the first image and the flux coming from all the other images.

In terms of the deflection angle parameters  $\bar{a}$  and  $\bar{b}$ , these observables can be written as<sup>71</sup>

$$\mathcal{S} = \theta_\infty e^{\bar{b}/\bar{a} - 2\pi/\bar{a}} \quad (83)$$

$$\mathcal{R} = e^{2\pi/\bar{a}} \quad (84)$$

The above equations (83) and (84) can be inverted to express  $\bar{a}$  and  $\bar{b}$  in terms of the image separation  $\mathcal{S}$  and the flux ratio  $\mathcal{R}$ . Therefore the knowledge of these two observables can be used to reconstruct the deflection angle given by Eq.(71). The aim of strong field gravitational lensing is to detect the relativistic images corresponding to specific lensing candidates and measure their separations and flux ratios. Once this is accomplished, the observed data could be compared with the theoretical coefficients obtained using various metrics. A precise set of observational data for strong gravitational lensing, if obtained, could therefore be able discriminate between different models of gravity. In the braneworld scenario the computation of the above parameters has been performed for two metrics<sup>29</sup> taking the black hole at the centre of our galaxy as a potential candidate.

We will now consider examples of the various lensing quantities defined above for some of the possible braneworld black hole geometries discussed in section 2. It is instructive to compare the braneworld lensing quantities with the standard Schwarzschild ones which for strong gravitational lensing are given as follows<sup>71</sup>. Choosing the Schwarzschild radius  $r_s = 2M/M_4^2$  as the unit of distance, the photon sphere is given by

$$r_{ph} = \frac{3}{2} \quad (85)$$

for Schwarzschild lensing. The corresponding minimum impact parameter is

$$u_m = \frac{3\sqrt{3}}{2} \quad (86)$$

The coefficients  $\bar{a}$  and  $\bar{b}$  defined in Eqs.(72) and (73) are given by

$$\bar{a} = 1 \quad (87)$$

$$\bar{b} = -\pi + 2\log[6(2 - \sqrt{3})] + \log[6] \quad (88)$$

The deflection angle (71) is obtained in terms of the parameters  $\bar{a}$  and  $\bar{b}$  to be<sup>71</sup>

$$\alpha(\theta) = -\log\left(\frac{2\theta D_d}{3\sqrt{3}} - 1\right) + \log[216(7 - 4\sqrt{3})] - \pi \quad (89)$$

In the weak field limit, the expression for the bending angle is given by

$$\alpha_{weak} = \frac{4M}{M_4^2 r_0} \quad (90)$$

For the analysis of gravitational lensing by braneworld metrics, let us first consider the Garriga-Tanaka weak field solution<sup>6</sup> given by Eq.(2) in isotropic coordinates. The metric in terms of the standard coordinates can be written as

$$ds_4^2 = - \left( 1 - \frac{2M}{M_4^2 r} + \frac{4Ml^2}{3M_4^2 r^3} \right) dt^2 + \left[ \frac{1 + \frac{M}{M_4^2 r} - \frac{Ml^2}{3M_4^2 r^3}}{1 + \frac{2M}{M_4^2 r} + \frac{2Ml^2}{3M_4^2 r^3}} \right]^{-2} dr^2 + r^2(d\Omega^2) \quad (91)$$

The formal expression for the radius of the photon sphere  $r_{ph}$  can be obtained as a function of  $M$  and  $l$  using Eq.(60) to be

$$r_{ph} = \frac{r_s}{2} + \frac{3^{1/3}r_s^2}{2(3r_s^3 - 20l^2r_s + 2\sqrt{10}\sqrt{10l^4r_s^2 - 3l^2r_s^4})^{1/3}} + \frac{(3r_s^3 - 20l^2r_s + 2\sqrt{10}\sqrt{10l^4r_s^2 - 3l^2r_s^4})^{1/3}}{23^{1/3}} \quad (92)$$

where  $r_s = 2M/M_4^2$ . However, it can be seen from Eq.(92) that no real solution for  $r_{ph}$  exists for admissible values of  $l$  and  $r_s$ . This is to be expected since the metric (2) represents a weak field solution. The weak field limit of the bending angle was obtained to be<sup>26</sup>

$$\alpha_{weak} = \frac{4M}{M_4^2 \tilde{r}_0} + \frac{4Ml^2}{M_4^2 \tilde{r}_0^3} \quad (93)$$

where  $\tilde{r}_0$  in this case is the isotropic coordinate equivalent of the distance of closest approach  $r_0$  in standard coordinates.

The analysis of strong field gravitational lensing can however be performed in other braneworld geometries. For example, let us consider lensing in the metric with tidal charge (5) given by<sup>14</sup>

$$dS_4^2 = - \left( 1 - \frac{2M}{M_4^2 r} + \frac{Q}{r^2} \right) dt^2 + \left( 1 - \frac{2M}{M_4^2 r} + \frac{Q}{r^2} \right)^{-1} dr^2 + r^2(d\Omega^2) \quad (94)$$

which resembles the Reissner-Nordstrom metric, but with  $Q < 0$  in the braneworld context. Again using units of distance  $2M/M_4^2$ , it is straightforward to obtain the expressions for the photon sphere and the minimum impact parameter given by<sup>71</sup>

$$r_{ph} = \frac{(3 + \sqrt{9 - 32Q})}{4} \quad (95)$$

$$u_m = \frac{(3 + \sqrt{9 - 32Q})^2}{4\sqrt{2}\sqrt{3 - 8Q + \sqrt{9 - 32Q}}} \quad (96)$$

The coefficients  $\bar{a}$  and  $\bar{b}$  in the deflection angle are given by<sup>71</sup>

$$\bar{a} = \frac{r_{ph}\sqrt{r_{ph} - 2Q}}{\sqrt{(3 - r_{ph})r_{ph}^2 - 9Qr_{ph} + 8Q^2}} \quad (97)$$

$$\begin{aligned} \bar{b} = -\pi + 2\log[6(2 - \sqrt{3})] + \frac{8Q(\sqrt{3} - 4 + \log[6(2 - \sqrt{3})])}{9} \\ + \frac{(r_{ph} - Q)^2[(3 - r_{ph})r_{ph}^2 - 9Qr_{ph} + 8Q^2]\bar{a}\log[2]}{(r_{ph} - 2Q)^3(r_{ph}^2 - r_{ph} + Q)} \end{aligned} \quad (98)$$

In terms of the above coefficients one obtains the complete expression for the deflection angle using Eq.(71). The weak field limit of the bending angle was derived to be<sup>26</sup>

$$\alpha_{weak} = \left( \frac{1}{M_4^2} - \frac{3\pi Q}{16Mr_0} \right) \frac{4M}{r_0} \quad (99)$$

Note that the bending angle is always positive because of negative tidal charge  $Q$  unlike the electric charge of the Reissner-Noredstrom metric.

We next consider the braneworld solution (9) in terms of the PPN parameter  $\beta$  given by<sup>36</sup>

$$ds_4^2 = -(1 - \frac{2M}{M_4^2 r})dt^2 + \frac{1 - \frac{3M}{2M_4^2 r}}{(1 - \frac{2M}{M_4^2 r})(1 - \frac{M(4\beta-1)}{2M_4^2 r})} + r^2(d\Omega^2) \quad (100)$$

For the above metric the expressions for the radius of the photon sphere  $r_{ph}$  and the minimum impact parameter are of course similar to those for Schwarzschild lensing given by Eqs.(85) and (86), as is easy to see using Eqs.(59), (60) and (61). The expression for the deflection angle can be derived in terms of the coefficients  $\bar{a}$  and  $\bar{b}$  which for the metric (100) are given by (setting the unit of distance as  $2M/M_4^2$ )

$$\bar{a} = \frac{\sqrt{3}}{\sqrt{6 - (4\beta - 1)}} \quad (101)$$

$$\bar{b} = -\pi + \frac{2\sqrt{3}}{\sqrt{6 - (4\beta - 1)}}\log[6(2 - \sqrt{3})] + \frac{\sqrt{3}}{\sqrt{6 - (4\beta - 1)}}\log[6] \quad (102)$$

Kar and Sinha<sup>26</sup> obtained the weak field limit of the bending angle for the metric (100) to be

$$\alpha_{weak} = \frac{2M(1 + \beta)}{r_0} \quad (103)$$

Note that the standard Schwarzschild expressions are recovered in Eqs.(101), (102) and (103), as should be, for  $\beta = 1$ .

The lensing observables  $\mathcal{S}$  and  $\mathcal{R}$  corresponding to the ratio between the flux of the first image and the flux coming from all the other images as defined in Eqs.(83) and (84) respectively, can be computed using the expressions for  $u_m$ ,  $\bar{a}$ , and  $\bar{b}$  for

particular geometries. One can obtain the magnitudes of  $\mathcal{S}$  and  $\mathcal{R}$  for particular lensing candidates using the known values for their masses and distances. For the black hole located at the centre of our galaxy at a distance of  $D_d = 8.5\text{kpc}$  and with mass  $M = 2.8 \times 10^6 M_\odot$ , the position of relativistic images in Schwarzschild strong lensing was first computed by Virbhadra and Ellis<sup>72</sup>, and the observable parameters  $\mathcal{S}$  and  $\mathcal{R}$  were computed by Bozza<sup>71</sup>. Whisker<sup>29</sup> has computed using the above black hole as a candidate lens the values for these observables for two possible braneworld geometries given by the metric (94) with tidal charge<sup>14</sup> and another solution<sup>44</sup>.

Table 1. Estimates for the strong field lensing angle coefficients and observables for the black hole at the center of our galaxy with mass  $M = 2.8 \times 10^6 M_\odot$  and  $D_d = 8.5$  kpc, for standard Schwarzschild and two different braneworld geometries. ( $r_m = 2.5\log\mathcal{R}$ .)

Observables	Schwarzschild metric	Brane metric with tidal charge $Q$			Brane metric with PPN parameter $\beta$	
		$Q = -0.1$	$Q = -0.2$	$Q = -0.3$	$\beta = 1 + 10^{-4}$	$\beta = 1 - 10^{-4}$
		16.87	17.87	18.92	19.65	16.87
$\theta_\infty(\mu \text{ arc sec})$	0.0211	0.0142	0.0102	0.097	0.02115	0.01923
$r_m(\text{magnitudes})$	6.82	7.02	7.2	7.37	6.818	6.887
$u_m/r_s$	2.6	2.75	2.9	3	2.6	2.6
$\bar{a}$	1	0.9708	0.938	0.925	1.00006	0.9999
$\bar{b}$	-0.4002	-0.612	-0.747	-0.819	-0.402	-0.429

In Table 1 we display the values of these lensing quantities  $\theta_\infty, \mathcal{S}, \mathcal{R}, u_m/r_s, \bar{a}$ , and  $\bar{b}$  first for Schwarzschild lensing. We compare the values of the lensing observables with those obtained for lensing with two braneworld geometries, i.e., the metric (94) with tidal charge<sup>14</sup>, and the metric (100) with the PPN parameter  $\beta$ <sup>36</sup>. We choose three negative values of the tidal charge  $Q$ . The two values of the parameter  $\beta$  on either side of the Schwarzschild value ( $\beta = 1$ ) are chosen to maintain observational compatibility with the solar system tests of the Nortvedt effect<sup>37</sup>. The measurement of the observable  $\theta_\infty$  involves a microsecond resolution which should in principle be attainable by the very long baseline interferometry projects such as MAXIM<sup>77</sup>. Though the actual identification of faint relativistic images would be extremely difficult in practice due to the inherent disturbances<sup>72</sup>, an accurate measurement of  $\theta_\infty$  would be able to distinguish the Schwarzschild geometry from the braneworld RN-type one. However, to unambiguously determine the exact nature of the black hole through the lensing angle coefficients  $\bar{a}$  and  $\bar{b}$ , one has to measure the observables  $\mathcal{S}$  and  $\mathcal{R}$ . Since this involves the resolution of two faint images separated by  $\sim 0.02\mu \text{ arc sec}$ , such an observation would need a leap of technological development over the present astronomical facilities<sup>29,71</sup>.

Let us finally return to the Myers-Perry metric (13) which is obtained from the 5-dimensional Schwarzschild metric<sup>15</sup> and could be relevant for the geometry near the horizon of a small  $r \leq l$  braneworld black hole. The cosmological evolution of

such black holes formed in the early universe having the metric

$$dS_4^2 = - \left( 1 - \frac{r_{BH}^2}{r^2} \right) dt^2 + \left( 1 - \frac{r_{BH}^2}{r^2} \right)^{-1} dr^2 + r^2 (d\Omega^2) \quad (104)$$

has been described in details in section 4. It is possible for such black holes to survive through the intermediate eras of the universe<sup>20,21</sup>. It is feasible that such black holes with masses in the sub-lunar range exist as dark matter in galactic haloes<sup>24,23</sup>. The photon sphere for a Myers-Perry braneworld black hole in units of  $2M/M_4^2$  is given by

$$r_{ph} = \frac{2}{\sqrt{3\pi}} \sqrt{\frac{l}{l_4}} \sqrt{\frac{M_4}{M}} \quad (105)$$

and is plotted as a function of black hole mass in Figure 2. The minimum impact parameter is

$$u_m = \sqrt{2}r_{ph} \quad (106)$$

The coefficients  $\bar{a}$  and  $\bar{b}$  given by<sup>28</sup>

$$\bar{a} = \frac{1}{\sqrt{2}} \quad (107)$$

$$\bar{b} = -\pi + \sqrt{2} \log(4\sqrt{2}) \quad (108)$$

can be then be used to construct the strong field deflection angle. Eiroa<sup>28</sup> has calculated the positions and magnifications of the relativistic images and compared them with those of Schwarzschild black holes.

Gravitational lensing in the weak field limit by the black hole (104) has been worked out<sup>27</sup>. When the impact parameter  $u$  exceeds a few times the horizon radius given by Eq.(28), but is still lesser than  $l$  ( $u \leq l$ ), the application of weak field

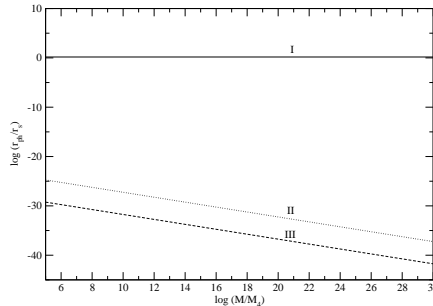


Fig. 2. The photon sphere  $r_{ph}$  (in units of the Schwarzschild radius  $r_s$ ) is plotted versus mass for the Schwarzschild black hole (I), and the Myers-Perry braneworld black holes with  $l = 10^{30}l_4$  (II), and  $l = 10^{20}l_4$  (III).

lensing could be relevant. The weak field limit of the deflection angle was calculated to be<sup>27</sup>

$$\alpha_{\text{weak}} = \frac{2Mll_4}{M_4 r_0^2} \quad (109)$$

In order to satisfy the requirement that  $u \leq l$ , and also obtain non-negligible magnification at the image location, the mass of the black hole should be such that<sup>27</sup>

$$\frac{M}{M_4} \leq \frac{l}{l_4} \quad (110)$$

Using the maximum allowed value for  $l$  by present experiments<sup>8</sup>, one then obtains that  $M \leq 10^{-8} M_\odot$ . So weak field gravitational lensing for such a black hole could be applicable only for masses in the sub-lunar range. As discussed above the braneworld scenario is conducive to the existence of primordial black holes in the sublunar mass range<sup>20,21</sup>. If such black holes exist in our galactic halo, then the magnification of their weak field images turns out to be diminished compared to the standard Schwarzschild black holes of similar mass<sup>27</sup>.

Table 2. Estimates for the strong field lensing angle coefficients and observables for a black hole in the galactic halo with mass  $M = 10^{25}$  gm and  $D_d = 10^{22}$  cm, for the standard Schwarzschild and the Myers-Perry geometry with two different values of  $l$ . ( $r_m = 2.5 \log \mathcal{R}$ .)

Observables	Myers-Perry metric with extra dimension $l$		Schwarzschild metric
	$l = 10^{30} l_4$	$l = 10^{20} l_4$	
$\theta_\infty$ ( $\mu$ arc sec)	$0.039 \times 10^{-12}$	$0.0123 \times 10^{-16}$	$0.03 \times 10^{-12}$
$\mathcal{S}$ ( $\mu$ arc sec)	$0.2042 \times 10^{-17}$	$0.0644 \times 10^{-21}$	$0.0375 \times 10^{-15}$
$r_m$ (magnitudes)	9.64	9.64	6.82
$u_m/r_s$	3.37	$1.065 \times 10^{-4}$	2.6
$\bar{a}$	0.707	0.707	1
$\bar{b}$	-0.689	-0.689	-0.4002

Before concluding this section we present a comparative study of lensing in the Myers-Perry geometry (104) with that in the standard Schwarzschild geometry. The respective photon spheres are plotted as a function of mass in Figure 2 choosing two values of  $l$  for the braneworld case. The mass range chosen is the one which could be relevant for Myers-Perry braneworld black holes (104) that have been conjectured to exist in the form of binaries in the galactic halo<sup>23,24</sup>. Choosing a specific value of mass in the above range, the strong field lensing quantities have been evaluated separately for the above two metrics. The strong lensing angle coefficients  $\bar{a}$  and  $\bar{b}$ , and the observables  $\theta_\infty$ ,  $\mathcal{R}$  and  $\mathcal{S}$  are displayed in Table 2. It is interesting to note that a larger value for the scale of the extra dimension  $l$  takes the values of the observables  $\theta_\infty$  and  $\mathcal{S}$  for the braneworld case closer to those of Schwarzschild lensing. This happens because the size of the braneworld black hole which is much smaller compared to the Schwarzschild black hole of same mass increases with  $l$  for fixed mass (28). Of course, the values of these lensing quantities are far beyond the

possibility of verification by present observational capabilities. But the comparison of these numbers provides an in principle method of discriminating between different gravity models.

## 6. Summary and Conclusions

Braneworld black holes are the potential testing arenas of a rich theoretical structure associated with modified braneworld gravity and extra dimensions. If the fundamental scale of gravity is much lower than the 4-dimensional Planck scale, then it is feasible for higher dimensional black holes to be formed in low energy processes. A lot of the present interest in the prospect of obtaining observable signatures of braneworld gravity is via the properties of the evaporation products of mini black holes produced either in particle collisions inside accelerators<sup>9,10</sup>, or in high energy cosmic ray showers<sup>11</sup>. Another issue of interest is regarding primordial black holes which may be formed through the collapse of overdense regions in the braneworld high energy phase of the early universe. Such black holes could have diverse cosmological implications. Further, even larger black holes could form by gravitational collapse of matter on the brane. Braneworld black holes have entirely different metrics compared to 4-dimensional black holes, and carry the signature of the extra dimension in their geometries. The focus of this review has been to discuss the cosmological consequences of primordial braneworld black holes, and also to analyse the features associated with gravitational lensing in several braneworld black hole metrics.

The physics of gravitational collapse on the brane is not yet understood in totality<sup>13</sup>. A serious conceptual difficulty arises due to the fact that the gravitational field equations are rendered incomplete on the brane by the effect of the bulk gravitational modes. No complete solution to the bulk gravitational field equations representing a spherically symmetric vacuum black hole metric on the brane has been found till date. Projections of the 5-dimensional Weyl tensor have been used in the 4-dimensional brane field equations in various configurations to obtain possible braneworld black hole metrics. In section 2 we have discussed some possible candidate geometries for braneworld black holes. These metrics are in general rather different from the standard Schwarzschild metric, and incorporate modifications of the standard  $1/r$  gravitational potential in braneworld gravity<sup>6</sup>. The braneworld black hole solutions contain interesting features related to the existence of horizons, and the modified black hole entropy and temperature. The Reissner-Nordstrom type solution<sup>14</sup> contains a negative tidal charge which can be viewed as the reflection of the black hole mass by the bulk with negative cosmological constant. Other solutions discussed include the one that incorporates the contribution of the projected Weyl tensor in terms of the post-Newtonian parameters<sup>36</sup>.

The 5-dimensional character of braneworld gravity at small scales motivates the consideration of the induced Myers-Perry metric<sup>15</sup> as a braneworld black hole candidate for black holes with radius  $r < l$ . Physically this corresponds to the fact that a

small black hole is unable to distinguish between the bulk dimension and our 3 brane dimensions. The modified properties<sup>16</sup> of such black holes within the braneworld context have been discussed<sup>47</sup>, and the different subtleties regarding their Hawking evaporation on the brane and into the bulk have been analysed earlier<sup>17</sup>. Special features of the interaction of 5-dimensional black holes with the brane have been revealed in the literature<sup>18,25,48,49,78</sup>. In this review we have highlighted the relevance of using the Myers-Perry geometry for the analysis of the processes of Hawking evaporation and the accretion of radiation in the early cosmological evolution of primordial black holes in the braneworld scenario.

In section 3 we have provided a short summary of the main features of the cosmology in the RS-II model<sup>4</sup>. Essentially the cosmology in the early braneworld era (high energy brane regime) is altered by the presence of a term in the Friedmann equation on the brane that is quadratic in the energy momentum tensor. This modifies the Hubble expansion at times earlier than the time  $t_c \equiv l/2$ . Among other consequences, such a scenario allows for the possibility of inflation with steep potentials that could be excluded in the standard scenario. Various features of the cosmology of braneworld models have been analysed in details in some recent reviews<sup>1,5</sup>. In the context of the present review, the most significant implication of the modified high energy behaviour is that the expansion of the Hubble volume makes it feasible for accretion by the primordial black holes of the surrounding radiation to take place. This feature is primarily responsible for the mass growth and prolonged survival<sup>20,21</sup> of the braneworld black holes. The standard cosmological expansion of the universe is recovered at later times, in order for the observationally established processes such as nucleosynthesis to work out.

The description of the braneworld cosmological evolution with primordial black holes has been provided in section 4. The modified mass-radius relationship for the induced 4-dimensional Myers-Perry black holes leads to slower evaporation and longer lifetimes compared to standard Schwarzschild black holes<sup>19</sup>. The detailed properties of evaporation of such black holes are described in a recent review<sup>17</sup>. The accretion of radiation in the high energy phase could be effective because the growth of black hole mass is smaller than the growth of the mass in the Hubble volume in braneworld evolution<sup>20,21</sup>. Thus, a large fraction of primordial black holes may survive up to much later eras. The decaying black holes affect several cosmological processes at different eras, and hence the observational abundance of different species, for example, the background high energy photons<sup>65</sup>, could be used to put constraints on the initial mass spectrum of the black holes. These constraints have to be evaluated considering the altered cosmological evolution in the braneworld scenario, and therefore could be significantly modified compared to similar constraints in standard cosmology<sup>22</sup>. The exchange of energy of the black holes with the surrounding radiation in the high energy era leads to mass disequilibration of neighbouring black holes<sup>23</sup>. As a consequence, binaries could be formed later through 3-body gravitational interactions. Such binaries have masses in the sub-lunar range, and gravitational waves emitted during their coalescence come in the

detectable range<sup>24</sup>.

Braneworld black holes existing at present times offer another scope of detection, viz. through the gravitational lensing of light sources by them. In section 5 we have first briefly reviewed the framework of gravitational lensing using which both weak field and strong field lensing can be handled in a unified manner<sup>71</sup>. The expressions for the lensing quantities in different braneworld metrics have been presented analysing the crucial differences from standard Schwarzschild lensing. Myers-Perry black holes existing in the galactic halo in certain mass ranges would be difficult to detect via weak field lensing due to reduced magnification compared to Schwarzschild black holes<sup>27</sup>. Strong field gravitational lensing through its prominent features such as the production of relativistic images and retrolensing offers the ultimate scope of discriminating between different gravity models<sup>28</sup>. Using the black hole at the centre of our galaxy as a candidate lens, it is possible to compute the theoretical values of several lensing observables in different geometries<sup>29</sup>. We have presented the computed lensing observables for a few braneworld metrics. A comparison with the lensing observables of the Schwarzschild metric shows that it might be possible to distinguish the braneworld black hole with tidal charge<sup>14</sup> from the Schwarzschild black hole by the possible measurement of one of these observables in the near future.

The physics of extra dimensions is no longer a field of mere theoretical constructs. There is currently a lot of ongoing activity on finding observational signatures of braneworld black holes through different physical mechanisms. In addition to the motion of light rays, the properties of massive orbiting particles in these geometries are also expected to exhibit interesting features. In particular, it has been shown that no stable circular orbits exist in the equatorial plane of the Myers-Perry metric<sup>78</sup>. The position of the innermost stable orbit shifts for braneworld black holes as is the case with the photon sphere, and this could lead to observable modifications of the properties of the accretion disks around black holes. Gravity wave spectroscopy offers another possibility of observing braneworld gravity. It has been pointed out using the black string between two branes as a model of a braneworld black hole, that the massive bulk gravity modes could lead to detectable spectroscopic signatures that are absent in the normal 4-dimensional gravitational waves<sup>79</sup>. Furthermore, the possibility of even distinguishing between different braneworld models such as the ADD model<sup>2</sup> and the RS model<sup>14</sup> via the production of their respective black holes in accelerators has been argued<sup>80</sup>. Much excitement exists indeed in the prospects of detecting signatures of extra dimensions. The range of cosmological and astrophysical implications of extra dimensions, braneworld gravity, and black holes have only started to be investigated.

## References

1. R. Maartens, *Living Rev. Rel.* **7**, 1 (2004).
2. N. Arkani-Hamed, S. Dimopoulos and G. R. Dvali, *Phys. Lett. B* **429**, 263 (1998); I. Antoniadis, N. Arkani-Hamed, S. Dimopoulos and G. Dvali, *Phys. Lett. B* **436**,

257 (1998); N. Arkani-Hamed, S. Dimopoulos and G. Dvali, Phys. Rev. D**59**, 086004 (1999).

3. L. Randall and R. Sundrum, Phys. Rev. Lett. **83**, 3370 (1999).
4. L. Randall and R. Sundrum, Phys. Rev. Lett. **83**, 4690 (1999).
5. P. Brax and C. van de Bruck, Class. Quant. Grav. **20**, R201 (2003).
6. J. Garriga and T. Tanaka, Phys. Rev. Lett. **84**, 2778 (2000).
7. S. B. Giddings, E. Katz and L. Randall, JHEP **0003**, 023 (2000).
8. C. D. Hoyle, U. Schmidt, B. R. Heckel, E. G. Adelberger, J. H. Gundlach, D. J. Kapner and H. E. Swanson, Phys. Rev. Lett. **86**, 1418 (2001); J. C. Long, H. W. Chan, A. B. Churnside, E. A. Gulbis, M. C. M. Varney and J. C. Price, Nature **421**, 922 (2003).
9. D. M. Eardley and S. B. Giddings, Phys. Rev. D**66**, 044011 (2002); K. Cheung, Phys. Rev. Lett. **88**, 221602 (2002).
10. S. Dimopoulos and G. Landsberg, Phys. Rev. Lett. **87**, 161602 (2001); L. Anchordoqui and H. Goldberg, Phys. Rev. D**67**, 064010 (2003); M. Cavaglia, S. Das and R. Maartens, Class. Quant. Grav. **20**, L205 (2003); A. Chamblin, F. Cooper and G. C. Nayak, Phys. Rev. D**69**, 065010 (2004).
11. J. L. Feng and A. D. Shapere, Phys. Rev. Lett. **88**, 021303 (2002); L. Anchordoqui and H. Goldberg, Phys. Rev. D**65**, 047502 (2002); M. Ave, E.-J. Ahn, M. Cavaglia, and A.V. Olinto, Phys. Rev. D**68**, 043004 (2003).
12. T. Shiromizu, K. Maeda and M. Sasaki, Phys. Rev. D**62**, 024012 (2000).
13. C. Germani, M. Bruni and R. Maartens, Phys. Rev. Lett. **87**, 231302 (2001); T. Tanaka, Prog. Theor. Phys. Suppl. **148**, 307 (2002); R. Emparan, A. Fabbri and N. Kaloper, JHEP **08**, 043 (2002).
14. N. Dadhich, R. Maartens, P. Papadopoulos and V. Rezania, Phys. Lett. B**487**, 1 (2000).
15. R. C. Myers and M. J. Perry, Ann. Phys. **172**, 304 (1986).
16. P. Argyres, S. Dimopoulos, J. March-Russel, Phys. Lett. B**441**, 96 (1998).
17. P. Kanti, Int. J. Mod. Phys. A**19**, 4899 (2004).
18. V. Frolov and D. Stojkovic, Phys. Rev. D**66**, 084002 (2002); V. Frolov and D. Stojkovic, Phys. Rev. Lett. **89**, 151302 (2002).
19. R. Guedens, D. Clancy and A. R. Liddle, Phys. Rev. D**66**, 043513 (2002).
20. A. S. Majumdar, Phys. Rev. Lett. **90**, 031303 (2003).
21. R. Guedens, D. Clancy and A. R. Liddle, Phys. Rev. D**66**, 083509 (2002).
22. D. Clancy, R. Guedens and A. R. Liddle, Phys. Rev. D**68**, 023507 (2003).
23. A. S. Majumdar, A. Mehta and J. M. Luck, Phys. Lett. B**607**, 219 (2005).
24. K. T. Inoue and T. Tanaka, Phys. Rev. Lett. **91**, 021101 (2003).
25. V. Frolov, M. Snajdr and D. Stojkovic, Phys. Rev. D**68**, 044002 (2003).
26. S. Kar and M. Sinha, Gen. Rel. Grav. **35**, 10 (2003).
27. A. S. Majumdar and N. Mukherjee, astro-ph/0403405.
28. E. F. Eiroa, gr-qc/0410128.
29. R. Whisker, Phys. Rev. D**71**, 064004 (2005).
30. M. Sasaki, T. Shiromizu and K. Maeda, Phys. Rev. D**62**, 024008 (2000).
31. A. Chamblin, S. W. Hawking and H. S. Reall, Phys. Rev. D**61**, 065007 (2000).
32. E. Anderson and J. E. Lidsey, Class. Quant. Grav. **18**, 4831 (2001); C. Barcelo, R. Maartens, C. F. Sopuerta and F. Viniegra, Phys. Rev. D**67**, 064203 (2003).
33. R. Gregory, Class. Quant. Grav. **17**, L125 (2000).
34. N. Dadhich, Phys. Lett. B**492**, 357 (2000).
35. N. Dadhich and S. G. Ghosh, Phys. Lett. B**518**, 1 (2001).
36. R. Casadio, A. Fabbri and L. Mazzacurati, Phys. Rev. D**65**, 084040 (2002).
37. C. M. Will, Living. Rev. Rel. **4**, 4 (2001).

38. C. Germani and R. Maartens, Phys. Rev. **D64**, 124010 (2001).
39. N. Dadhich, S. Kar, S. Mukherjee and M. Visser, Phys. Rev. **D65**, 064004 (2002).
40. K. A. Bronnikov and S. W. Kim, Phys. Rev. **D67**, 064027 (2003); K. A. Bronnikov, V. N. Melnikov and H. Dehnen, Phys. Rev. **D68**, 024025 (2003).
41. S. Shankaranarayanan and N. Dadhich, Int. J. Mod. Phys. **D13**, 1095 (2004).
42. A. N. Aliev and A. E. Gumrukcuoglu, hep-th/0502223.
43. G. Kofinas, E. Papantonopoulos and I. Pappa, Phys. Rev. **D66**, 104014 (2002); G. Kofinas, E. Papantonopoulos and V. Zamarias, Phys. Rev. **D66**, 104028 (2002); M. Visser and D. L. Wiltshire, Phys. Rev. **D67**, 104004 (2003); T. Harko and M. K. Mak, Phys. Rev. **D69**, 064020 (2004); T. Harko and M. K. Mak, gr-qc/0503072.
44. R. Gregory, R. Whisker, K. Beckwith and C. Done, JCAP **10**, 013 (2004).
45. K. Nakao, K. Nakamura and T. Mishima, Phys. Lett. **B564**, 143 (2003); C-M. Yoo, K. Nakao and D. Ida, gr-qc/0503008.
46. H. Kudoh, T. Tanaka and T. Nakamura, Phys. Rev. **D68**, 024035 (2003).
47. E. Emparan, G. Horowitz, R. Myers, JHEP **0001**, 007 (2000).
48. V. Frolov and D. Stojkovic, Phys. Rev. **D67**, 084004 (2003).
49. V. Frolov, D. Fursaev and D. Stojkovic, JHEP **0406**, 057 (2004); V. Frolov, D. Fursaev and D. Stojkovic, Class. Quant. Grav. **21**, 3483 (2004).
50. D. Stojkovic, JHEP **0409**, 061 (2004).
51. T. Shiromizu and M. Shibata, Phys. Rev. **D62**, 127502 (2000); A. Chamblin, H. S. Reall, H. A. Shinkai and T. Shiromizu, Phys. Rev. **D63**, 064015 (2001).
52. T. Wiseman, Phys. Rev. **D65**, 124007 (2002).
53. P. Kanti and K. Tamvakis, Phys. Rev. **D65**, 084010 (2002); P. Kanti, I. Olasagasti and K. Tamvakis, Phys. Rev. **D68**, 124001 (2003); R. Casadio and L. Mazzacurati, Mod. Phys. Lett. **A18**, 651 (2003).
54. P. Binetruy, C. Deffayet, U. Ellwanger and D. Langlois, Phys. Lett. **B477**, 285 (2000); D. Langlois, R. Maartens, M. Sasaki and D. Wands, Phys. Rev. **D63**, 084009 (2001); J. D. Barrow and R. Maartens, Phys. Lett. **B532**, 153 (2002).
55. J. E. Lidsey, Lect. Notes. Phys. **646**, 357 (2004).
56. J. M. Cline, C. Grojean and G. Servant, Phys. Rev. Lett. **83**, 4245 (1999); R. Maartens, D. Wands, B. A. Bassett and I. P. C. Heard, Phys. Rev. **D62**, 041301 (2000); G. Huey and J. E. Lidsey, Phys. Lett. B **514**, 217 (2001); R. Maartens, V. Sahni and T. D. Saini, Phys. Rev. **D63**, 063509 (2001); S. Mizuno, K. Maeda, K. Yamamoto, Phys. Rev. **D67**, 024033 (2003); K. Kunze, Phys. Lett. **B587**, 1 (2004).
57. E. J. Copeland, A. R. Liddle and J. E. Lidsey, Phys. Rev. **D64** 023509 (2001); A. S. Majumdar, Phys. Rev. **D64**, 083503 (2001); V. Sahni, M. Sami and T. Souradeep, Phys. Rev. **D65**, 023518 (2002); N. J. Nunes and E. J. Copeland, Phys. Rev. **D66**, 043524 (2002); A. R. Liddle and L. A. Urena-Lopez, Phys. Rev. **D68**, 043517 (2003); K. Dimopoulos, Phys. Rev. **D68**, 123506 (2003); M. Sami, N. Dadhich and T. Shiromizu, Phys. Lett. **B568**, 118 (2003); H. Tashiro, T. Chiba and M. Sasaki, Class. Quant. Grav. **21**, 1761 (2004); M. Sami and V. Sahni, Phys. Rev. **D70**, 083513 (2004); S. Mizuno, S.-J. Lee and E. J. Copeland, Phys. Rev. **D70**, 043525 (2004).
58. S. Nojiri and S. D. Odintsov, JHEP **0007**, 049 (2000); C. Charmousis and J. F. Dufaux, Class. Quant. Grav. **19**, 4671 (2002); S. C. Davis, Phys. Rev. **D67**, 024030 (2003); K. Maeda and T. Torii, Phys. Rev. **D69**, 024002 (2004); J. F. Dufaux, J. E. Lidsey, R. Maartens and M. Sami, Phys. Rev. **D70**, 083525 (2004).
59. S. Nojiri, S. D. Odintsov and S. Ogushi, Int. J. Mod. Phys. **A17**, 4809 (2002); J. E. Lidsey and N. J. Nunes, Phys. Rev. **D67**, 103510 (2003); S. Tsujikawa, M. Sami and R. Maartens, Phys. Rev. **D70**, 063525 (2004); M. Sami, N. Savchenko and A. Toporensky, Phys. Rev. **D70**, 123528 (2004).

60. A. S. Majumdar, P. Das Gupta and R. P. Saxena, *Int. J. Mod. Phys. D* **4**, 517 (1995); N. Upadhyay, P. Das Gupta and R. P. Saxena, *Phys. Rev. D* **60**, 063513 (1999).
61. P. S. Custodio and J. E. Horvath, *Phys. Rev. D* **58**, 023504 (1998); P. S. Custodio and J. E. Horvath, *Phys. Rev. D* **60**, 083002 (1999).
62. A. A. Starobinsky, *JETP Lett.* **55**, 489 (1992); B. J. Carr and J. E. Lidsey, *Phys. Rev. D* **48**, 543 (1993); A. M. Green and A. R. Liddle, *Phys. Rev. D* **56**, 6166 (1997); K. Jedamzik and J. C. Niemeyer, *Phys. Rev. D* **59**, 124014 (1999); A. M. Green and A. R. Liddle, *Phys. Rev. D* **60**, 063509 (1999); G. D. Kribs, A. K. Leibovich and I.Z. Rothstein, *Phys. Rev. D* **60**, 103510 (1999); T. Bringmann, C. Keifer and D. Polarski, *Phys. Rev. D* **65**, 024008 (2002); D. Blais, T. Bringmann, C. Keifer and D. Polarski, *Phys. Rev. D* **67**, 024024 (2003).
63. T. Nakamura, M. Sasaki, T. Tanaka and K. S. Thorne, *Astrophys. J.* **487**, L139 (1997); K. Ioka, T. Chiba, T. Tanaka and T. Nakamura, *Phys. Rev. D* **58**, 063003 (1998).
64. R. Bean and J. Magueijo, *Phys. Rev. D* **66**, 063505 (2002); P. S. Custodio and J. E. Horvath, *gr-qc/0502118*.
65. Y. Sendouda, S. Nagataki and K. Sato, *Phys. Rev. D* **68**, 103510 (2003).
66. Y. Sendouda, K. Kohri, S. Nagataki and K. Sato, *astro-ph/0408369*.
67. S. Orito et al, *Phys. Rev. Lett.* **84**, 1078 (2000); T. Maeno et al, *Astropart. Phys.* **16**, 121 (2001).
68. P. Schneider, J. Ehlers and E. E. Falco, *Gravitational Lenses*, (Springer, 1992).
69. For a review, see. F. Bernardeau, [*astro-ph/990117*] in *Theoretical and Observational Cosmology*, ed. M. Lachieze-Rey (Cargese Summer School, 1998).
70. V. Bozza, S. Capozziello, G. Iovane and G. Scarpetta, *Gen. Rel. Grav.* **33**, 1535 (2001).
71. V. Bozza, *Phys. Rev. D* **66**, 103001 (2002).
72. K. S. Virbhadra and G. F. R. Ellis, *Phys. Rev. D* **62**, 084003 (2000).
73. K. S. Virbhadra and G. F. R. Ellis, *Phys. Rev. D* **65**, 103004 (2002); A. O. Petters, *MNRAS* **338**, 457 (2003); V. Bozza and L. Mancini, *Gen. Rel. Grav.* **36**, 435 (2004).
74. D. E. Holtz and J. A. Wheeler, *Astrophys. J.* **587**, 330 (2002); F. De Paolis, A. Geralico, G. Ingrosso and A. A. Nucita, *Astron. Astrophys.* **409**, 809 (2003).
75. E. F. Eiroa and D. F. Torres, *Phys. Rev. D* **69**, 063004 (2004).
76. V. Bozza and L. Mancini, *Astrophys. J.* **611**, 1045 (2004).
77. MAXIM web page: <http://maxim.gsfc.nasa.gov/>
78. V. Frolov and D. Stojkovic, *Phys. Rev. D* **68**, 064011 (2003); M. K. Mak and T. Harko, *Phys. Rev. D* **70**, 024010 (2004).
79. S. S. Seahra, C. Clarkson and R. Maartens, *gr-qc/0408032*.
80. D. Stojkovic, *Phys. Rev. Lett.* **94**, 011603 (2005).